Original Research Article

A Hydrodynamic Model of Flow in Bifurcating Streams, Part 2: Effects of Environmental Thermal Differentials

Abstract This paper presents a hydrodynamic model of flow in a bifurcating stream, in which the effects of environmental thermal differentials are investigated. The governing equations are solved analytically using similarity transformation and perturbation series expansions methods. The solutions for the temperature, velocity and concentration are obtained and analyzed quantitatively and graphically. The results show that the heat exchange parameter reduces the velocity of the flow, and this enhances early deposition of the stream bed loads. Furthermore, it is seen that free convection force increases the flow velocity, thus serving as a cushion for the adverse effect of heat exchange parameter on the flow.

Keywords: *bifurcating stream, hydrodynamic model, thermal differentials, similarity transformation, perturbation method*

1 INTRODUCTION

In part one of this study, we considered the hydrodynamic flow of a bifurcating stream for the case where the effects of bifurcation angle and nature of the source rocks are significant. In the part one, the effects of environmental thermal differentials are played down. Therefore, we are motivated to examine the effects of the temperature differentials on the flow.

There are some reports from previous research works on the flow in bifurcating systems. For example, [1], [2] and [3] in their various studies observed that bifurcation angle increases the inlet pressure in the daughter channel, which consequently increases the flow velocity. [4] studied the flow in a bifurcating fine porous capillaries, and noticed that magnetic field has a freezing effect on the flow velocity structure.

The paper shall be organized in the following format: section 2 is the material and method; section 3 the results and discussion, and section 4 the conclusions.

2. MATERIALS AND METHODS

There is always a temperature difference between the internal/ambient temperature of the stream and that at its surface called the external or environmental temperature condition. This temperature differential referred to as the heat exchange parameter can be described in terms of the Newton's law of cooling as $\frac{\partial \theta}{\partial y} = h(\theta_{ext} - \theta_{\text{int}})$ where h is the film heat transfer coefficient which could be negative. The magnitude of the temperature at the surface of the stream is influenced by the climatic condition of the region where it is found. In particular, the environmental temperature depends tremendously on the radiation from the sun. The higher the radiation the higher it becomes. When the environmental temperature is higher than the equilibrium temperature of the stream, heat flows from the surface into it, that is, the stream absorbs heat from the environmental source. The effects the heat absorption can be seen in the energization of the water particles.

We assume the stream bifurcates symmetrically as shown in Figure 1 in part one of the studies, and that the flow is axi-symmetrical about the z-axis. Therefore, if (u', v') are respectively the velocity components of the fluid in the mutually orthogonal (x', y') axes, then the mathematical equations of mass balance/continuity, momentum, energy and diffusion governing the flow, considering the Boussinesq approximations, we have:

$$\frac{\partial u'}{\partial x'} + \frac{\partial v'}{\partial y'} = 0 \tag{1}$$

$$u'\frac{\partial u'}{\partial x'} + v'\frac{\partial u'}{\partial y'} = -\frac{1}{\rho}\frac{\partial p'}{\partial x'} + \frac{\mu}{\rho}\left(\frac{\partial^2 u'}{\partial x'} + \frac{\partial^2 u'}{\partial y'}\right) \tag{2}$$

$$u'\frac{\partial v'}{\partial x'} + v'\frac{\partial v'}{\partial y'} = -\frac{1}{\rho}\frac{\partial p'}{\partial y'} + \frac{\mu}{\rho}\left(\frac{\partial^2 v'}{\partial x'} + \frac{\partial^2 v'}{\partial y'}\right) \tag{3}$$

$$u'\frac{\partial T'}{\partial x'} + v'\frac{\partial T'}{\partial y'} = -\frac{1}{\rho}\frac{k_o}{C_p}\left(\frac{\partial^2 T'}{\partial x'^2} + \frac{\partial^2 T'}{\partial y'^2}\right) + \frac{1}{\rho}\frac{Q}{C_p}\left(T' - T_\infty\right) \tag{4}$$

$$u\frac{\partial C'}{\partial x'} + v'\frac{\partial C'}{\partial y'} = -\frac{D}{\rho}\left(\frac{\partial^2 C'}{\partial x'^2} + \frac{\partial^2 C'}{\partial y'^2}\right) + \frac{k_r^2}{\rho}\left(C' - C_\infty\right) \tag{5}$$

The model examines the dynamics of a bifurcating stream flowing from a point $x' = -\infty$ towards a shore at $x' = x_o$, as seen in Figure 1. The model shows that the channel is assumed to be symmetrical and divided into two regions: the upstream (or mother) region $x' < x_o$ and downstream (or daughter) region $x' > x_o$, where x_o is the bifurcation or the nodal point, which is assumed to be the origin such that the stream boundaries become $y' = \pm d$ for the upstream region and $y' = \alpha x'$ for the downstream region. Due to geometrical transition between the mother and daughter channels, the problem of wall curvature effect is bound to occur. To fix up this, a very simple transition wherein the width of the daughter channel is made equal to half that of the mother channel i.e. $\pm d$ such that the variation of the bifurcation angle is straight-forwardly used (see [3]). Furthermore, if the width of the stream ($2d$) is far less than its length (l_o) before the point of bifurcation such that the ratio of $\frac{2d}{l_o} = \Re << 1$, (where $\Re$ is the aspect ratio), the flow is laminar and Poiseuille (see [5]). d is assumed to be non-dimensionally equal to one (see [3]). Similarly, at the entry region of the mother channel, the flow velocity is given as $u' = U_o\left(1 - y'^2\right)$, where U_o is the characteristic velocity, which is taken to be maximum at the centre and zero at the wall (see [3]). Based on the fore-going, the boundary conditions are:

$$\text{u}'=1,\ \text{v}'=0,\ \text{T}'=1,\ \text{C}'=1 \quad \text{at} \quad \text{y}'=0 \tag{6}$$

$$\text{u}'=1,\ \text{v}'=0,\ \text{T}'=1,\ \text{C}'=1 \quad \text{at} \quad \text{y}'=0 \tag{7}$$

for the mother channel

$$\text{u}'=0,\ \text{v}'=0,\ \text{T}'=0,\ \text{C}'=0 \quad \text{at y} =0 \tag{8}$$

$$\text{u}'=0,\ \text{v}'=0,\ \text{T}'=\gamma \text{T}_\text{w},\ \text{C}'=\gamma C_\text{w},\ \gamma_1 < 1,\ \gamma_2 < 1 \quad \text{at y}' = \alpha x' \tag{9}$$

for the daughter channel

Introducing the dimensionless variables and similarity transformations, we have

$$f'' = 0 \tag{10}$$

$$f''' + f'' - M_1^2 f' + \mathrm{Re}(f' f'' + ff'') = -Gr\,\Theta - Gc\,\Phi \tag{11}$$

$$\Theta'' + \Theta' + \mathrm{Re}\,\mathrm{Pr}(-f'\Theta' + f\,\Theta') + N^2\Theta = 0 \tag{12}$$

$$\Phi'' + \Phi' + R\,eSc(-f'\Phi' + f\,\Phi') + \delta_1^2\Phi = 0 \tag{13}$$

with the boundary indications:

$$f = 1, f' = 0, \Theta = 1, \Phi = 1 \quad \text{at } \eta = 0 \tag{14}$$

$$f' = 0, f = 0, \Theta = \Theta_w, \Phi = \Phi_w \quad \text{at } \eta = 1 \tag{15}$$

for the mother channel

$$f = 0, f' = 0, \Theta = 0, \Phi = 0 \quad \text{at } \eta = 0 \tag{16}$$

$$f' = 0, f = 0, \Theta = \gamma_1\Theta_w, \Phi = \gamma_2\Phi_w,\ \gamma_1 < 1, \gamma_2 < 1 \quad \text{at } \eta = ax \tag{17}$$

for the daughter channel

where

$$M_1^2 = (\chi^2 + M^2)$$

$$x = \frac{x'}{\ell_c},\ y = \frac{y'}{\ell_c},\ u = \frac{u'}{U_o},\ v = \frac{v'}{U_o},\ p = \frac{p'}{p_\infty},\ \rho_\infty = \rho U_o^2,\ \Theta = \frac{T' - T_\infty}{T_w - T_\infty},$$

$$\Phi = \frac{C' - C_\infty}{C_w - C_\infty},\ \upsilon = \frac{\rho}{\mu}, \mathrm{Re} = \frac{\rho U_o \ell_c}{\mu}, Gr = \frac{\rho g \beta_t (T_w - T_\infty)\ \ell_c^2}{\mu U_o}, Gc = \frac{\rho g \beta_c (C_w - C_\infty)}{\mu U_o},$$

$$\chi^2 = \frac{\ell^2{}_c}{\kappa},\ \delta_1^2 = \frac{k_r^2 \ell_c^2}{D},\ M^2 = \frac{\sigma_e B_o^2\ \ell_c^2}{\rho\mu\mu_m}, N^2 = \frac{C_p\mu}{k_o}, Sc = \frac{\mu}{\rho D},$$

are the dimensionless variables,

$$\Psi = (U_o \upsilon\, x)^{1/2} f(\eta),\quad \eta = \left(\frac{U_o}{\upsilon x}\right)^{1/2} y \tag{18}$$

the similarity transformations,

$$u = \frac{\partial\Psi}{\partial y},\ v = -\frac{\partial\Psi}{\partial x} \tag{19}$$

the velocity components,

and β_t and β_c are the volumetric expansion coefficient for temperature and concentration respectively; p' is the pressure; C_∞ concentration at equilibrium; T_∞ temperature at equilibrium; κ is the permeability parameter of the porous medium; B_o^2 is the applied uniform magnetic field strength due the nature of the fluid; σ_e is the electrical conductivity of the fluid; k_o the thermal conductivity; C_p the specific heat capacity at constant pressure; Q is the heat absorption coefficient; k_r^2 is the rate of chemical reaction of the fluid, which is homogeneous and of order one; C' concentration (quantity of material being transported); D diffusion coefficient; **g** gravitational field vector; T' fluid temperature; ρ density of the fluid; μ viscosity of the fluid; μ_m magnetic permeability of the fluid; υ kinematic viscosity; k_o thermal conductivity of the medium; ℓ_c is the scale length; U_o characteristic or reference velocity which is maximum at the centre and almost zero at the wall; C_w constant wall temperature is maintained; T_w constant wall concentration at which the channel is maintained; p_∞ is the ambient/equilibrium pressure; ρ_∞ the ambient/equilibrium density; υ is the kinematic viscosity; Re is the Reynolds number; Gr is the Grashof number due to temperature difference; Gc is the Grashof number due to concentration difference; χ^2 is the local Darcy number; M^2 is the Hartmann's number; Pr is the Prandtl number; Sc is the Schmidt number; and δ_1^2 is the rate of chemical reaction; N^2 is the temperature differential.

Equations (10) - (13) are coupled and highly non-linear. Therefore, to linearize and make them tractable, we introduce regular perturbation series solutions of the form:

$$h(x,y) = h_o(x,y)) + \xi h_1(x,y) + \ldots \qquad (20)$$

where $\xi = \frac{1}{\text{Re}} << 1$ Is the perturbing parameter. We choose this parameter because, almost at the point of bifurcation, due to a change in the geometrical configuration, the inertial force rises and the momentum increases. The increase in the momentum is associated with a drastic increase in the Reynolds number, indicating a sort of turbulent flow. In this regard, equations (10) - (17) become:

for the zeroth order:

$$f_o'' = 0 \qquad (21)$$

$$f_o''' + f_o'' - M_1^2 f_o' = -Gr\Theta_o - Gc\Phi_o \qquad (22)$$

$$\Theta''_o + \Theta'_o + N^2\Theta_o = 0 \qquad (23)$$

$$\Phi_o'' + \Phi_o' + \delta^2{}_1\Phi_o = 0 \qquad (24)$$

with the boundary conditions

$$f_o = 1,\ f_o' = f_o'' = 0,\ \Theta_o = 1,\ \Phi_o = 1 \quad \text{at } \eta = 0 \qquad (25)$$

$$f_o = 0,\ f_o' = f_o'' = 0,\ \Theta_o = \Theta_w,\ \Phi_o = \Phi_w \quad \text{at } \eta = 1 \qquad (26)$$

for the first order:

$$f_1'' = 0 \qquad (27)$$

$$f_1''' + f_1'' - M_1^2 f_1' = f_o' f_o'' - f_o f_o'' - Gr\Theta_1 - Gc\Phi_1 \qquad (28)$$

$$\Theta_1'' + \Theta_1' + N^2\Theta_1 = \Pr(f_o'\Theta'_o - f_o\Theta'_o) \qquad (29)$$

$$\Phi_1'' + \Phi_1' + \delta_1^2\Phi_1 = Sc(f_o'\Phi_o' - f_o\Phi_o') \qquad (30)$$

with the boundary conditions

$$f_1 = 0, f_1' = 0, \Theta_1 = 0, \Phi_1 = 0 \quad \text{at } \eta = 0 \qquad (31)$$

$$f_1 = 0, f_1^{'} = 0, \Theta_1 = \gamma_1 \Theta_w, \Phi_1 = \gamma_2 \Phi_w,\ \gamma_1 < 1, \gamma_2 < 1 \quad \text{at} \quad \eta = ax \tag{32}$$

The zeroth order equations describe the flow in the upstream channel, while the first order equations describe the flow in the downstream channels. The zeroth order terms in the first order equations indicate the influence of the upstream on the downstream flow.

The solutions to equations (21) - (26) and (27) - (32) are:
for the mother channel

$$\Theta_o(\eta) = \frac{\Theta_w e^{\frac{1}{2}(1-\eta)} \sinh \mu_1 \eta}{\sinh \mu_1} + \frac{e^{-\frac{1}{2}(1-\eta)} \sinh \mu_1 (1-\eta)}{\sinh \mu_1} \tag{33}$$

$$\Phi_o(\eta) = \frac{\Phi_w e^{\frac{1}{2}(1-\eta)} \sinh \mu_2 \eta}{\sinh \mu_2} + \frac{e^{-\frac{1}{2}(1-\eta)} \sinh \mu_2 (1-\eta)}{\sinh \mu_2} \tag{34}$$

$$f_o(\eta) = \frac{\left(f_{o(p)}(0) e^{-(\mu 3+\eta/2)} \ \sinh \mu_3 \eta\right)}{\sinh \mu_3} + \frac{\left(f_{o(p)}(1) e^{-1/2(1-\eta)} \ \sinh \mu_3 \eta\right)}{\sinh \mu_3}$$

$$-f_{o(p)}(0) e^{-(\mu_3+\eta/2)} + f_{o(p)}(\eta) \tag{35}$$

and for the daughter region

$$\Theta_1(\eta) = \frac{\gamma_1 \Theta_w e^{\frac{1}{2}(\alpha x-\eta)} \sinh \mu_1 \eta}{\sinh(\mu_1 \alpha x)} - \frac{\Theta_{1(p)}(\alpha x) e^{-\frac{1}{2}(\alpha x-\eta)} \sinh \mu_1 \eta}{\sinh(\mu_1 \alpha x)}$$

$$+\frac{\Theta_{1(p)}(0) e^{-(\mu \alpha x+\eta/2)} \sinh \mu_1 \eta}{\sinh(\mu_1 \alpha x)} - \Theta_{1(p)}(0) e^{-(\alpha x-(\mu_1+1/2)\eta\ )} + \Theta_{1(p)}(\eta) \tag{36}$$

$$\Phi_1(\eta) = \frac{\gamma_2 \Phi_w e^{\frac{1}{2}(\alpha x-\eta)} \sinh \mu_2 \eta}{\sinh(\mu_2 \alpha x)} + \frac{\Phi_{1(p)}(\alpha x) e^{-\frac{1}{2}(\alpha x-\eta)} \sinh \mu_2 \eta}{\sinh(\mu_2 \alpha x)}$$

$$+\frac{\Phi_{1(p)}(0) e^{-(\mu \alpha x+\eta/2)} \sinh \mu_2 \eta}{\sinh(\mu_2 \alpha x)} - \Phi_{1(p)}(0) e^{-(\alpha x-(\mu_2+1/2)\eta\ )} + \Phi_{1(p)}(\eta) \tag{37}$$

$$f_1(\eta) = \frac{f_{1(p)}(0) e^{-(\mu_3 \alpha x+\eta/2)} \sinh \mu_3 \eta}{\sinh \mu_3 \alpha x} + \frac{f_{1(p)}(\alpha x) e^{1/2(\alpha x-\eta)} \sinh \mu_3 \eta}{\sinh(\mu_3 \alpha x)}$$

$$-f_{1(p)}(0) e^{(\alpha x-(\mu_{3+1/2})\eta)} + f_{1(p)}(\eta) \tag{38}$$

3 RESULTS AND DISCUSSION

Using Maple 12 computational software, we computed for various values of χ^2, N^2 and Gr/Gc to obtain the results shown below:

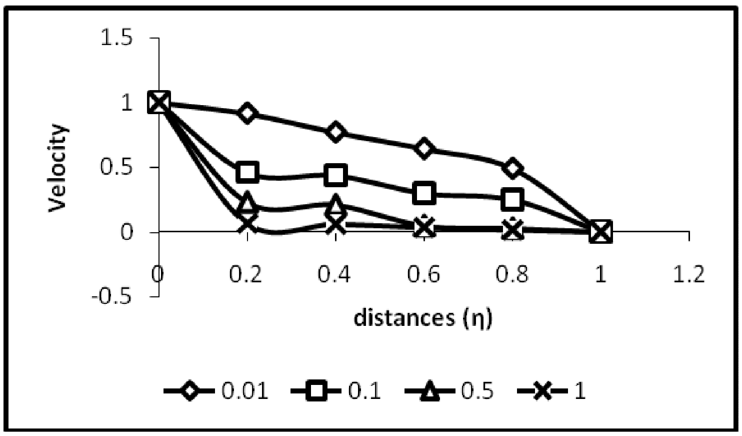

Figure 1 Velocity-porosity parameter (χ^2) profiles at various distances (η) in the mother channel

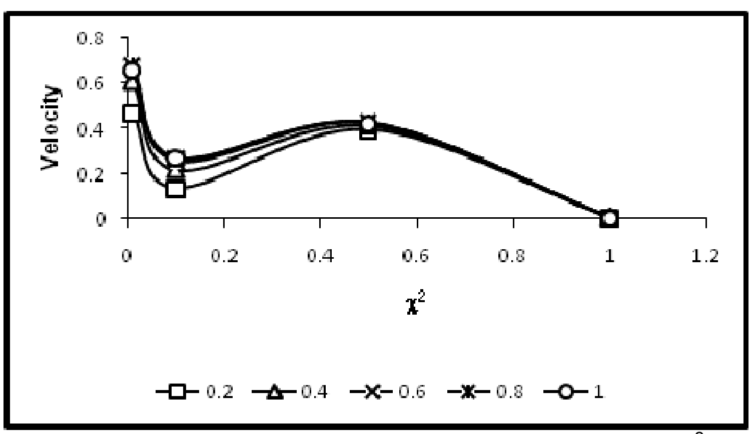

Figure 2 Velocity profiles for various porosity parameter (χ^2) in the daughter channel

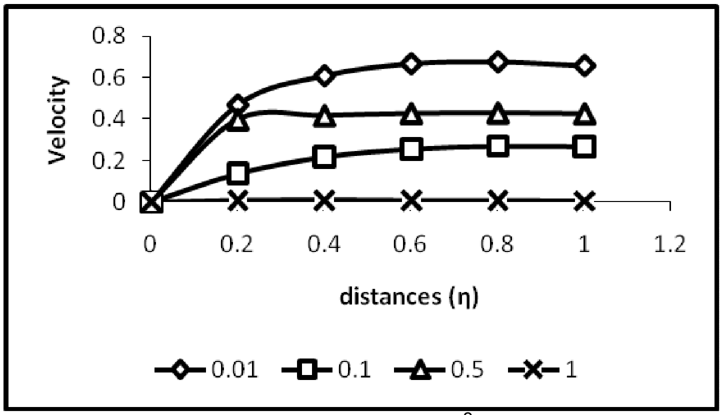

Figure 3 Velocity-porosity parameter (χ^2) profiles at various distances (η) in the daughter channel

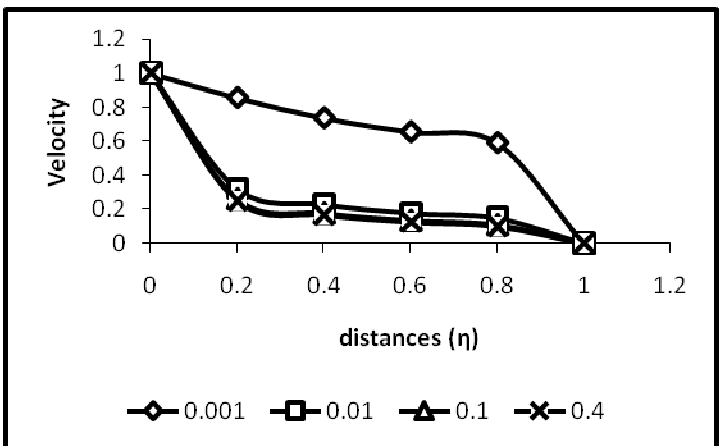

Figure 4 Velocity-heat exchange parameter (N^2) profiles at various distances (η) in the mother channel

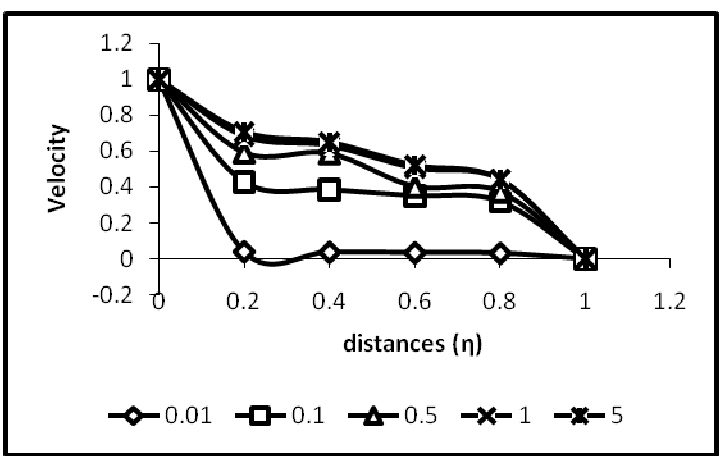

Figure 5 Velocity-Grashof number (Gr/Gc) profiles at various distances (η) in the mother channel.

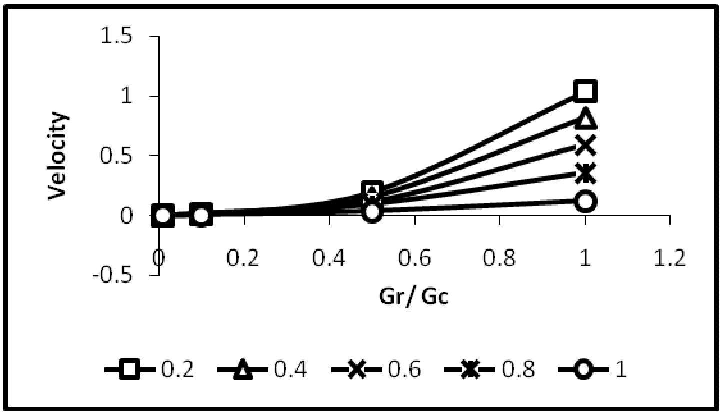

Figure 6 Velocity profiles for various Grashof numbers (Gr/Gc) in the daughter channel

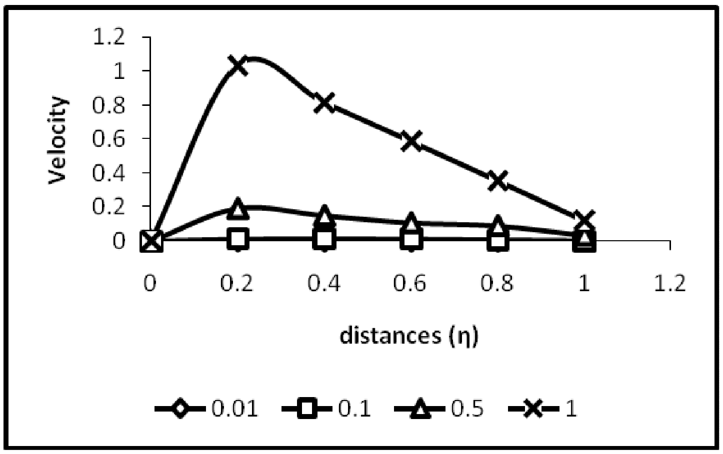

Figure 7 Velocity-Grashof numbers (Gr/Gc) profiles at various distances (η) in the daughter channel

The purpose of this paper is to investigate the effects of thermal differentials on the flow in a bifurcating stream. To this end, Figure1 – Figure 7 show the profiles of the computational results of the flow variables obtained for various values of χ_1^2 , N^2 and Gr/Gc. For realistic values of Pr =0.71, γ_1 = 0.6, γ_2 =0.6, γ =0.7, Φ_w = 2.0, Θ_w =2.0, $\delta_1^2 = 0.2$, M^2= 0.2, α =10, Re=400, and for varying values of and χ^2= 0.1, 0.5, 1.0, 10; N^2= 0.001, 0.01, 0.1, 0.4 and Gr/Gc=0.01, 0.1, 0.5, 1.0, 5, 10 the profiles indicate that the flow velocity decreases as χ^2 and N^2 increase but increases with Gr/Gc.

A high porosity of the stream bank may give room for a soak-away of the water. In the absence of a commensurate increase in the water supplied from the aquifers that feed the stream, its volume will decrease, and subsequently, its velocity which is maximum when the volume is high decreases. This may account for what is seen in Figure1. Also, the oscillatory motion (Figure 2 and Figure 3) leads to lose of energy for the axial transport velocity.

Furthermore, as the environmental temperature increases, the stream may lose its water through evaporation, and soak-away into the dry flood plain. Without adequate supplies from the aquifers its water level drops; hence its velocity decreases (see Figure 4). Generally, the decrease in the velocity increases the rate of sediments deposition on the stream bed, thus, making it shallow earlier as it flows toward a standing water body.

On the other hand, the free convection force/buoyancy force which arises from the thermal differential in the presence of gravity serves as a lifting force for the water particles; hence increases the flow velocity (Figure 5 –Figure 7). It is evident that the free convection force serves as a cushioning factor for the effects of porosity and heat exchange parameter on the stream transport velocity.

Similarly, the oscillatory and fluctuating motion, manifested in the form of back- and-forth movement of the water, as seen in Figure 6 and Figure 7, possibly, may be due to the internal waves developed in the water in the flow process, or may be caused by the interaction between the pressure forces and the gravity forces.

The increase and decrease in the velocity, coupled with the fluctuating motion have some great significance in the flow. The increase in velocity enhances the transport of the sediments farther towards the standing water bodies, thus saving the stream from early shallow-up. On the other hand, the decrease in velocity produces the contrary situation. Furthermore, the oscillatory and fluctuating motion leads to lose of energy for the flow in the axial direction, and this also adversely affect the transport of the bed loads.

4 CONCLUSION

The analyses of this model show that the porosity and heat exchange parameter decrease the flow velocity, while the free convection force increases it. In fact, the free convection force cushions the reducing-effects of porosity and heat exchange parameters on the flow velocity of the stream.

REFERENCES

[1] Smith FT. Steady flow through a branching tube, Process Soc. London. 1977; A355:167-187.

[2] Sobey J, Philip Drazin G. Bifurcating two- dimensional flow, J Fluid Mechanics. 1986; 171: 263 -287.

[3] Tadjfar M, Smith FT. Direct simulation and modeling of a 3- dimensional bifurcating tube flow. J Fluid Mechanics. 2004; 519:1- 32.

[4] Okuyade WIA. MHD blood flow in bifurcating porous fine capillaries. African J Science Research. 2015; 4(4): 56-59

[5] Bestman AR. Global models for the biomechanics of green plants, Part 1, International J Energy Research. 1991; 16: 677– 84.

APPENDICES

$$f_{o(p)}(\eta) = -\left(\frac{n_3}{n_3\left(n_3^2 - n_2 n_3\right)} - \frac{1}{\left(n_3^2 - n_2 n_3\right)}\right)\left(\frac{GrAe^{\lambda_1 \eta}}{\lambda_1} + \frac{GrBe^{\lambda_2 \eta}}{\lambda_2} + \frac{GrCe^{m_1 \eta}}{m_1} + \frac{GrDe^{m_2 \eta}}{m_2}\right)$$

$$+\frac{n_3}{n_3\left(n_3^2-n_2n_3\right)}\left(\frac{GrAe^{\lambda_1\eta}}{\left(\lambda_1-n_2\right)}+\frac{GrBe^{\lambda_2\eta}}{\left(\lambda_2-n_2\right)}+\frac{GrCe^{m_1\eta}}{\left(m_1-n_2\right)}+\frac{GrDe^{m_2\eta}}{\left(m_2-n_2\right)}\right)$$

$$-\frac{1}{n_3\left(n_3^2-n_2n_3\right)}\left(\frac{GrAe^{\lambda_1\eta}}{\left(\lambda_1-n_3\right)}+\frac{GrBe^{\lambda_2\eta}}{\left(\lambda_2-n_3\right)}+\frac{GrCe^{m_1\eta}}{\left(m_1-n_3\right)}+\frac{GrDe^{m_2\eta}}{\left(m_2-n_3\right)}\right)$$

$$\lambda_1=-\frac{1}{2}+\frac{\sqrt{1-4N^2}}{2},\ \lambda_2=-\frac{1}{2}-\frac{\sqrt{1-4N^2}}{2}$$

$$\lambda_1=-\frac{1}{2}+\mu_1,\lambda_2=-\frac{1}{2}-\mu_1,\mu_1=\frac{\sqrt{1-4N^2}}{2}$$

$$m_1=-\frac{1}{2}+\mu_2,m_2=-\frac{1}{2}-\mu_2,\mu_2=\frac{\sqrt{1-4\delta_1^2}}{2}$$

$$n_2=-\frac{1}{2}+\mu_3,n_3=-\frac{1}{2}-\mu_3,\mu_3=\frac{\sqrt{1-4M^2}}{2}$$

$$A=\frac{\Theta_w e^{1/2}-e^{\mu_1}}{\sinh\mu_1},B=\frac{e^{\mu_1}-\Theta_w e^{1/2}}{\sinh\ \mu_1},\ C=\frac{\Phi_w e^{1/2}-e^{\mu_2}}{\sinh\mu_2},D=\frac{e^{\mu_2}-\Phi_w e^{1/2}}{\sinh\mu_2}$$

$$\Theta_{1(p)}(\eta)=\frac{\Pr}{(\lambda_2-\lambda_1)}\Big[\ \lambda_1FAe^{(\lambda_1+n_2)\eta}+\lambda_1GAe^{(\lambda_1+n_3)\eta}$$

$$-\left(\frac{n_3}{n_2\left(n_3^2-n_2n_3\right)}-\frac{1}{\left(n_3^2-n_2n_3\right)}\right)\left(\begin{array}{l}GrA^2e^{2\lambda_1\eta}+\dfrac{\lambda_1GrABe^{(\lambda_1+\lambda_2)\eta}}{\lambda_2}+\dfrac{\lambda_1GcACe^{(\lambda_1+m_1)\eta}}{m_1}\\+\dfrac{\lambda_1GcADe^{(\lambda_1+m_2)\eta}}{m_2}\end{array}\right)$$

$$+\frac{n_3}{n_2\left(n_3^2-n_2n_3\right)}\left(\frac{\lambda_1GrA^2e^{2\lambda_1\eta}}{\left(\lambda_1-n_2\right)}+\frac{\lambda_1GrABe^{(\lambda_1+\lambda_2)\eta}}{\left(\lambda_2-n_2\right)}+\frac{\lambda_1GcACe^{(\lambda_1+m_1)\eta}}{\left(m_1-n_2\right)}+\frac{\lambda_1GcADe^{(\lambda_1+m_2)\eta}}{\left(m_2-n_2\right)}\right)$$

$$-\frac{1}{\left(n_3^2-n_2n_3\right)}\left(\frac{\lambda_1GrA^2e^{2\lambda_1\eta}}{\left(\lambda_1-n_3\right)}+\frac{\lambda_1GrABe^{(\lambda_1+\lambda_2)\eta}}{\left(\lambda_2-n_3\right)}+\frac{\lambda_1GcACe^{(\lambda_1+m_1)\eta}}{\left(m_1-n_3\right)}+\frac{\lambda_1GcADe^{(\lambda_1+m_2)\eta}}{\left(m_2-n_3\right)}\right)\Big]+$$

…

$$\Phi_{1(p)}(\eta)=\frac{Sc}{(m_2-m_1)}\Big[\;m_1FCe^{(m_1+n_2)\eta}+m_1GCe^{(m_1+n_3)\eta}$$

$$-\left(\frac{n_3}{n_2\left(n_3^2-n_2n_3\right)}-\frac{1}{\left(n_3^2-n_2n_3\right)}\right)\left(\begin{array}{l}\frac{m_1GrACe^{(\lambda_1+m_1)\eta}}{\lambda_1}+\frac{m_1GrBCe^{(\lambda_2+m_1)\eta}}{\lambda_2}+GcC^2e^{2m_1\eta}\\+\frac{m_1GcCDe^{(m_1+m_2)\eta}}{m_2}\end{array}\right)$$

$$+\frac{n_3}{n_2\left(n_3^2-n_2n_3\right)}\left(\frac{m_1GrACe^{(\lambda_1+m_1)\eta}}{(\lambda_1-n_2)}+\frac{m_1GrBCe^{(\lambda_2+m_1)\eta}}{(\lambda_2-n_2)}+\frac{m_1GcC^2e^{2m_1\eta}}{(m_1-n_2)}+\frac{m_1GcCDe^{(m_1+m_2)\eta}}{(m_2-n_2)}\right)$$

$$-\frac{1}{\left(n_3^2-n_2n_3\right)}\left(\frac{m_1GrACe^{(\lambda_1+m_1)\eta}}{(\lambda_1-n_3)}+\frac{m_1GrBCe^{(\lambda_2+m_1)\eta}}{(\lambda_2-n_3)}+\frac{m_1GcC^2e^{2m_1\eta}}{(m_1-n_3)}+\frac{m_1GcCDe^{(m_1+m_2)\eta}}{(m_2-n_3)}\right)\Big]$$

$+\ldots$

$$-Gr\;\Big\{\frac{J_1e^{n_1\eta}}{n_2}+\frac{J_2e^{n_2\eta}}{n_2}\;+\frac{\Pr}{(\lambda_2-\lambda_1)}\Big[\frac{\lambda_1FAe^{(\lambda_1+n_2)\eta}}{(\lambda_1+n_2)}+\frac{\lambda_1GAe^{(\lambda_1+n_3)\eta}}{(\lambda_1+n_3)}$$

$$-\left(\frac{n_3}{\left(n_3^2-n_2n_3\right)}-\frac{1}{\left(n_3^2-n_2n_3\right)}\right)\left(\frac{GrA^2e^{2\lambda_1\eta}}{2}+\frac{GrBAe^{(\lambda_1+\lambda_2)\eta}}{(\lambda_1+\lambda_2)}+\frac{\lambda_1GcCAe^{(\lambda_1+m_1)\eta}}{(\lambda_1+m_1)m_1}+\frac{\lambda_1GcDAe^{(\lambda_1+m_2)\eta}}{(\lambda_1+m_2)m_2}\right)$$

$$+\frac{n_3}{n_2\left(n_3^2-n_2n_3\right)}\left(\frac{GrA^2e^{2\lambda_1\eta}}{2(\lambda_1-n_2)}+\frac{\lambda_1GrBAe^{(\lambda_1+\lambda_2)\eta}}{(\lambda_2-n_2)(\lambda_1+\lambda_2)}+\frac{\lambda_1GcCAe^{(\lambda_1+m_1)\eta}}{(m_1-n_2)(\lambda_1+m_1)}+\frac{\lambda_1GcDAe^{(\lambda_1+m_2)\eta}}{(m_2-n_2)(\lambda_1+m_2)}\right)$$

$$-\frac{1}{\left(n_3^2-n_2n_3\right)}\left(\frac{GrA^2e^{2\lambda_1\eta}}{2(\lambda_1-n_3)}+\frac{\lambda_1GrBAe^{(\lambda_1+\lambda_2)\eta}}{(\lambda_2-n_3)(\lambda_1+\lambda_2)}+\frac{\lambda_1GcCAe^{(\lambda_1+m_1)\eta}}{(m_1-n_3)(\lambda_1+m_1)}+\frac{\lambda_1GcDAe^{(\lambda_1+m_2)\eta}}{(m_2-n_3)(\lambda_1+m_2)}\right)\Big]$$

$+\ldots\}$

$$f_{1(p)}(\eta)=\left(\frac{n_3}{n_2\left(n_3^2-n_2n_3\right)}-\frac{1}{\left(n_3^2-n_2n_2\right)}\right)\;\Big\{\;\Big[Fe^{n_2\eta}+Ge^{n_3\eta}$$

$$-\left(\frac{n_3}{n_2\left(n_3^2-n_2n_3\right)}-\frac{1}{\left(n_3^2-n_2n_3\right)}\right)\left(\frac{GrAe^{\lambda_1\eta}}{\lambda_1}+\frac{GrBe^{\lambda_2\eta}}{\lambda_2}+\frac{GcCe^{m_1\eta}}{m_1}+\frac{GcDe^{m_2\eta}}{m_2}\right)$$

$$+\frac{n_3}{n_2\left(n_3^2-n_2n_3\right)}\left(\frac{GrAe^{\lambda_1\eta}}{\left(\lambda_1-n_2\right)}+\frac{GrBe^{\lambda_2\eta}}{\left(\lambda_2-n_2\right)}+\frac{GcCe^{m_1\eta}}{\left(m_1-n_2\right)}+\frac{GcDe^{m_2\eta}}{\left(m_2-n_2\right)}\right)$$

$$-\frac{1}{\left(n_3^2-n_2n_3\right)}\left(\frac{GrAe^{\lambda_1\eta}}{\left(\lambda_1-n_3\right)}+\frac{GrBe^{\lambda_2\eta}}{\left(\lambda_2-n_3\right)}+\frac{GcCe^{m_1\eta}}{\left(m_1-n_3\right)}+\frac{GcDe^{m_2\eta}}{\left(m_2-n_3\right)}\right)\ ]+\ldots$$

$$-\frac{1}{\left(n_3^2-n_2n_3\right)}\left(\frac{GrAe^{\lambda_1\eta}}{\left(\lambda_1-n_3\right)}+\frac{GrBe^{\lambda_2\eta}}{\left(\lambda_2-n_3\right)}+\frac{GcCe^{m_1\eta}}{\left(m_1-n_3\right)}+\frac{GcDe^{m_2\eta}}{\left(m_2-n_3\right)}\right)\ ]$$

$$-\left(\frac{n_3}{\left(n_3^2-n_2n_3\right)}-\frac{1}{\left(n_3^2-n_2n_3\right)}\right)\left(\frac{GrA^2e^{2\lambda_1\eta}}{2}+\frac{GrBAe^{(\lambda_1+\lambda_2)\eta}}{\left(\lambda_1+\lambda_2\right)}+\frac{\lambda_1GcCAe^{(\lambda_1+m_1)\eta}}{\left(\lambda_1+m_1\right)m_1}+\frac{\lambda_1GcDAe^{(\lambda_1+m_2)\eta}}{\left(\lambda_1+m_2\right)m_2}\right)$$

$$+\frac{n_3}{n_2\left(n_3^2-n_2n_3\right)}\left(\frac{GrA^2e^{2\lambda_1\eta}}{2\left(\lambda_1-n_2\right)}+\frac{\lambda_1GrBAe^{(\lambda_1+\lambda_2)\eta}}{\left(\lambda_2-n_2\right)\left(\lambda_1+\lambda_2\right)}+\frac{\lambda_1GcCAe^{(\lambda_1+m_1)\eta}}{\left(m_1-n_2\right)\left(\lambda_1+m_1\right)}+\frac{\lambda_1GcDAe^{(\lambda_1+m_2)\eta}}{\left(m_2-n_2\right)\left(\lambda_1+m_2\right)}\right)$$

$$-\frac{1}{\left(n_3^2-n_2n_3\right)}\left(\frac{GrA^2e^{2\lambda_1\eta}}{2\left(\lambda_1-n_3\right)}+\frac{\lambda_1GrBAe^{(\lambda_1+\lambda_2)\eta}}{\left(\lambda_2-n_3\right)\left(\lambda_1+\lambda_2\right)}+\frac{\lambda_1GcCAe^{(\lambda_1+m_1)\eta}}{\left(m_1-n_3\right)\left(\lambda_1+m_1\right)}+\frac{\lambda_1GcDAe^{(\lambda_1+m_2)\eta}}{\left(m_2-n_3\right)\left(\lambda_1+m_2\right)}\right)\ ]$$

$$+\ldots\quad -Gc\ \left\{\frac{\mathrm{R}_1e^{m_1\eta}}{m_1}+\frac{\mathrm{R}_2e^{m_2\eta}}{m_2}\quad+\frac{Sc}{\left(m_2-m_1\right)}\left[\frac{m_1FCe^{(m_1+n_2)\eta}}{\left(m_1+n_2\right)}+\frac{m_1GCe^{(m_1+n_3)\eta}}{\left(m_1+n_3\right)}\right.\right.+$$

$$\left(\frac{n_3}{n_2\left(n_3^2-n_2n_3\right)}-\frac{1}{\left(n_3^2-n_2n_3\right)}\right)\left(\frac{m_1GrACe^{\left(m_1+\lambda_1\right)\eta}}{\lambda_1\left(m_1+\lambda_1\right)}+\frac{m_1GrBCe^{\left(m_1+\lambda_1\right)\eta}}{\lambda_2\left(m_1+\lambda_1\right)}+\frac{GcC^2e^{2m_1\eta}}{2m_1}+\frac{m_1GcDCe^{\left(m_1+m_2\right)\eta}}{m_2\left(m_1+m_2\right)}\right)$$

$$-\frac{n_3}{n_2\left(n_3^2-n_2n_3\right)}\left(\frac{m_1GrACe^{\left(m_1+\lambda_1\right)\eta}}{\left(\lambda_1-n_2\right)\left(m_1+\lambda_1\right)}+\frac{m_1GrBCe^{\left(m_1+\lambda_2\right)\eta}}{\left(\lambda_2-n_2\right)\left(m_1+\lambda_2\right)}+\frac{GcC^2e^{2m_1\eta}}{\left(m_1-n_2\right)2}+\frac{m_1GcDCe^{\left(m_1+m_2\right)\eta}}{\left(m_2-n_2\right)\left(m_1+m_2\right)}\right)$$

$$-\frac{1}{\left(n_3^2-n_2n_3\right)}\left(\frac{m_1GrACe^{(m_1+\lambda_1)\eta}}{(\lambda_1-n_3)(m_1+\lambda_1)}+\frac{m_1GrBCe^{(m_1+\lambda_2)\eta}}{(\lambda_2-n_3)(m_1+\lambda_2)}+\frac{GcC^2e^{2m_1\eta}}{(m_1-n_3)2}+\frac{m_1GcDCe^{(m_1+m_2)\eta}}{(m_2-n_3)(m_1+m_2)}\right)\ ]$$

$+\ldots]\}$

$$E=0 \qquad F=\frac{\left(f_{o(p)}(0)e^{-(\mu_3+1/2)}-f_{o(p)}(1)\right)e^{1/2}}{2\sinh\mu_3},$$

$$G=\frac{-\left(f_{o(p)}(0)e^{-(\mu_3+1/2)}-f_{o(p)}(1)\right)e^{1/2}}{2\sinh\mu_3}-f_{o(p)}(0)$$

$$J_1=\frac{e^{\alpha x/2}\left(\gamma_1\Theta_w-\Theta_{1(p)}(\alpha x)+\Theta_{1(p)}(0)e^{-(\mu_1+1/2)\alpha x}\right)}{2\sinh(\mu_1\alpha x)},$$

$$J_2=\frac{-e^{\alpha x/2}\left(\gamma_1\Theta_w-\Theta_{1(p)}(\alpha x)+\Theta_{1(p)}(0)e^{-(\mu_1+1/2)\alpha x}\right)}{2\sinh(\mu_1\alpha x)}-\Theta_{1(p)}(0)$$

$$R_1=\frac{e^{\alpha x/2}\left(\gamma_2\Phi_w-\Phi_{1(p)}(\alpha x)+\Phi_{1(p)}(0)e^{-(\mu_2+1/2)\alpha x}\right)}{2\sinh(\mu_2\alpha x)},$$

$$R_2=\frac{-e^{\alpha x/2}\left(\gamma_2\Phi_w-\Phi_{1(p)}(\alpha x)+\Phi_{1(p)}(0)e^{-(\mu_2+1/2)\alpha x}\right)}{2\sinh(\mu_2\alpha x)}-\Phi_{1(p)}(0)$$